Phonon anomalies and lattice dynamics in the superconducting oxychlorides $Ca_{2-x}CuO_2Cl_2$

Matteo d'Astuto,* Ikuya Yamada,† Paola Giura, Lorenzo Paulatto, and Andrea Gauzzi
Institut de Minéralogie et de Physique des Milieux Condensés (IMPMC), UMR CNRS 7590, Université Pierre et Marie Curie - case 115, 4, place Jussieu, 75252 Paris cedex 05, France

Moritz Hoesch‡ and Michael Krisch
European Synchrotron Radiation Facility, BP 220, F-38043 Grenoble Cedex, France

Masaki Azuma and Mikio Takano
Laboratory of Solid State Chemistry, Institute for Chemical Research, Kyoto University, Uji, Kyoto-fu, 611-0011 Japan
(Received 5 June 2013; published 24 July 2013)

We present a comprehensive study of the phonon dispersion in an underdoped, superconducting $Ca_{2-x}CuO_2Cl_2$ crystal. We interpret the results using lattice dynamical calculations based on a shell model, and we compare the results to other hole-doped cuprates, in particular, to the ones isomorphic to $La_{2-x}Sr_xCuO_4$ (LSCO). We found that an anomalous dip in the Cu-O bond stretching dispersion develops in oxychlorides with a simultaneous marked broadening of the mode. The broadening is maximum at $\approx[\pi/(2a)\ 0\ 0]$, which corresponds to the charge-modulation propagation vector. Our analysis also suggests that screening effects in calculations may cause an apparent cosine-shaped bending of the Cu-O bond-stretching dispersion along both the (q 0 0) and (q q 0) directions, which is not observed on the data close to optimal doping. This observation suggests that the discrepancy between experimental data and *ab initio* calculations on this mode originates from an overestimation of the doping effects on the mode.

DOI: 10.1103/PhysRevB.88.014522 PACS number(s): 74.72.Gh, 63.20.D−, 63.20.kd, 78.70.Ck

I. INTRODUCTION

The discovery of high-temperature superconductivity (HTS) in cuprates was originally motivated by the search for superconductors with strong electron-phonon coupling.[1] The first HTS compounds, $La_{2-x}Ba_xCuO_4$ (LBCO) and LSCO, do indeed display a very large isotopic effect for oxygen, although the doping dependence of this effect turns out to be very anomalous.[2] Later studies pointed out that electron-phonon coupling may not be the main origin of the Cooper pairing,[3] in particular, for optimal doping. However, its role across the phase diagram of cuprates is still controversial, in particular, in its underdoped region. An important point is that single-electron band approximations, such as density functional theory (DFT) find a small electron-phonon coupling,[4,5] but they possibly miss many-body effects, as it was suggested that large couplings may exist in the presence of strong electron-electron correlations.[6]

An important point stressed in DFT-based investigations on electron-phonon coupling in cuprates is that these calculations seem to reproduce well the marked softening with a cosine dispersion, which develops under doping for longitudinal Cu-O bond-stretching mode along the direction (q 0 0) of such bonds (modes with Δ_1 character). At the same time, large discrepancies between those calculations for the same mode, but along the diagonal direction (q q 0) (modes with Σ_1 character), are found.[4,7] It has been suggested that the physical origin of the anomaly in the dispersion of the Cu-O bond-stretching modes is different for the two directions.[4,5]

Underdoped cuprates exhibit a static, or quasistatic, modulation of the charge, characterized by a stripe pattern parallel to the Cu-O bonds, which can give clear diffraction peaks both in the charge[8,9] and spin channel, for doping close to $\delta \sim 1/8$ with a propagation vector of $\approx\pi/(2a)$, i.e., a periodicity of $\approx 4a$, where a is the lattice parameter along the Cu-O bonds. Besides the above mentioned Cu-O bond stretching anomaly with cosine shape, an additional marked dip and a sizable broadening of the line shape is observed for the same phonon branch, close to the wave stripe vector $\mathbf{q} = (0.25,0,0)$;[10–14] it has been established that such feature can not be simulated by DFT.[15]

Large electron-phonon coupling can drive both phonon softening and broadening as it has been established, for example, in the case of classical superconductors such as, e.g., Nb[16] and, more recently, in YNi_2B_2C.[17] For cuprates, the issue remains controversial. In order to elucidate this aspect, we investigate the lattice dynamics in superconducting, underdoped $Ca_{2-x}CuO_2Cl_2$, using inelastic x-ray scattering (IXS) and compare our results with lattice dynamics calculations based on a shell model.

Doping $Ca_2CuO_2Cl_2$ oxychloride systems leads to a new family of HTS superconductors with T_c up to 43 K.[18,19] Their layered structure is similar to the cuprate one, characterized by CuO_2 planes, but without oxygen in the blocks separating these planes (see Fig. 1, left panel). These compounds represent an ideal test bench for the physics governing the high T_c superconductivity, which is commonly believed to depend only on the CuO_2 planes, independently from the details of the oxide blocks between them. In particular, oxychlorides have a chlorine ion that replaces the apical oxygen. The apical oxygen is important for the dynamics of the anionic octahedra surrounding the copper cation on most of the hole-doped cuprates. Moreover, oxychlorides are ideal for studying phonon dispersions, particularly the one of the copper-oxygen bond stretching mode by means of IXS spectroscopy, because they are composed only of low Z elements, thus yielding a higher IXS signal, due to the weaker photoelectric absorption compared to the cuprates, and also thanks to their simple

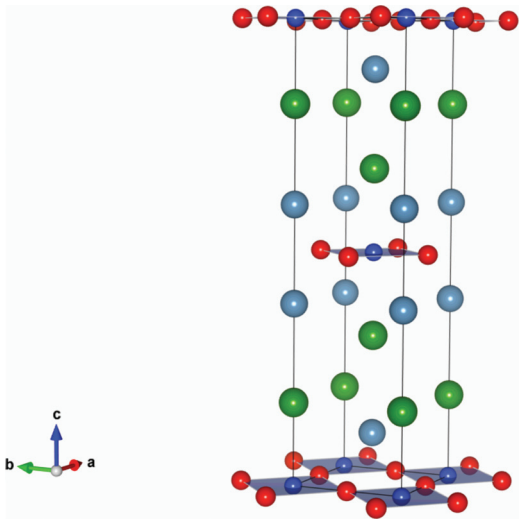

FIG. 1. (Color online) Drawing[21] of the unit cell of $Ca_2CuO_2Cl_2$.[22] The square coordination of copper with its four nearest-neighbor oxygen ions in the CuO_2 planes is shown. The chlorine ions are located in the apical site above the copper.

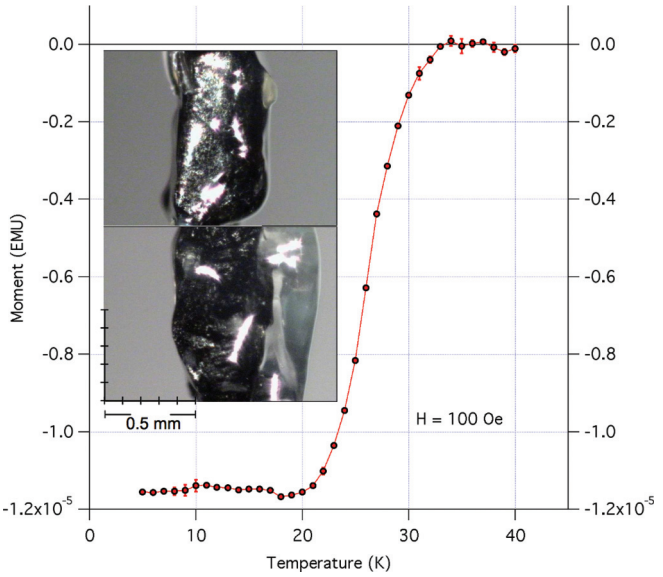

FIG. 2. (Color online) Chart[25] of the magnetization vs temperature across the superconducting transition at 100 Oe for the sample 2b measured by IXS. (Inset) Front and side views of the crystal, as measured in diffraction and IXS, in a grease film, with the glass fiber holder.

one-layer structure with small disorder, which reduces the number of modes to be measured and calculated. We note that these characteristics should also facilitate *ab initio* calculations. Underdoped oxychlorides show a modulation in the charge density, as their cuprate counterpart. However, this modulation is observed only in real space, using scanning tunelling microscopy (STM),[20] with a periodicity of $\approx 4a$ as for the stripes, but, up to now, not in diffraction.

In this work, we present a study of the phonon dispersion in superconducting $Ca_{2-x}CuO_2Cl_2$ doped with Ca vacancies. The study is as complete as possible, considering limitation from the crystal mosaic for the particular technique used (IXS), and the limited beam-time available on such highly specialized synchrotron experiment. We interpret the results using lattice dynamical calculations based on a shell model, and we compare our results to those obtained for other hole-doped cuprates, in particular the ones isomorphic to LSCO (T structure).[14,23,24] We found that an anomalous dip in the Cu-O bond stretching dispersion develops also in oxychlorides with a simultaneous marked broadening of the mode. The maximum of the broadening appears at the charge-modulation propagation vector of $\approx[\pi/(2a)\ 0\ 0]$. In addition to this effect, by comparing our results on the longitudinal Cu-O bond-stretching mode in superconducting $Ca_{2-x}CuO_2Cl_2$ to our model, we found that screening effect may lead to a simultaneous bending down of the whole dispersion along both the $(q\ 0\ 0)$ and $(q\ q\ 0)$ directions.

II. METHODS

A. Crystal growth and characteristics

We studied three different crystals of $Ca_{2-x}CuO_2Cl_2$, selected from several ones, with sizes of the order of 0.5 to 1 mm, from different batches, after a screening of their superconducting and crystalline properties as measured by the Meißner effect in a superconducting quantum interference device (SQUID) magnetometer (Quantum design MPMS©) and the diffraction on a four-circle diffractometer equipped with a Mo K_α anode, a κ-type goniometer, and a charge-coupled device (CCD) detector (Oxford diffraction Xcalibur©). We selected two of the crystals with nominal Ca vacancies doping $x = 0.2$, grown at high temperature (1250 °C) and high pressure (5.5 GPa),[19,22] and a parent insulating $Ca_2CuO_2Cl_2$ with stoichiometric composition. The best one, sample 2b, used for all the measurements of *in-plane* dispersion, of about 0.1-mm^3 volume (see Fig. 2), shows a superconducting transition temperature onset at $T_c^{\text{onset}} = 33$ K, with a well defined diamagnetic jump on a temperature window $\Delta T \approx 8$ K from 10% to 90% of the magnetization, as shown in Fig. 2. This corresponds to an underdoped compound with a Ca deficiency $x \sim 0.16 \pm 0.01$, slightly lower than the nominal one. The sample was protected from moist by a film of grease (Apizon N©) in order to avoid formation of hydroxides, during all the measurements. The grease film was also used to hold it on the borosilicate glass sample holder for diffraction and inelastic x-ray scattering (IXS), as shown in Fig. 2 (inset). The second doped crystal, named 1b, has also a nominal vacancy doping $x = 0.2$, similar crystalline and superconducting properties.

B. Inelastic x-ray scattering

The sample 2b was mounted in a vacuum chamber with Kapton©windows, with the scattering plane [(1,1,0),(0,0,1)] for measurements along (1,1,0) and [(1,0,0),(0,1,0)] for measurements along (1,0,0). The angular width of the (200) Bragg reflection rocking curve was 0.01° FWHM, proving excellent single-crystal quality *in-plane*. The second sample, 1b, was mounted with the direction (0,0,1) in the plane of scattering, but it revealed a large mosaic in the c^* direction, preventing us from completing the measurements along (0,0,1). This also prevented us for doing measurements on modes with *in-plane* propagation but *out-of-plane* polarization as, notably, the

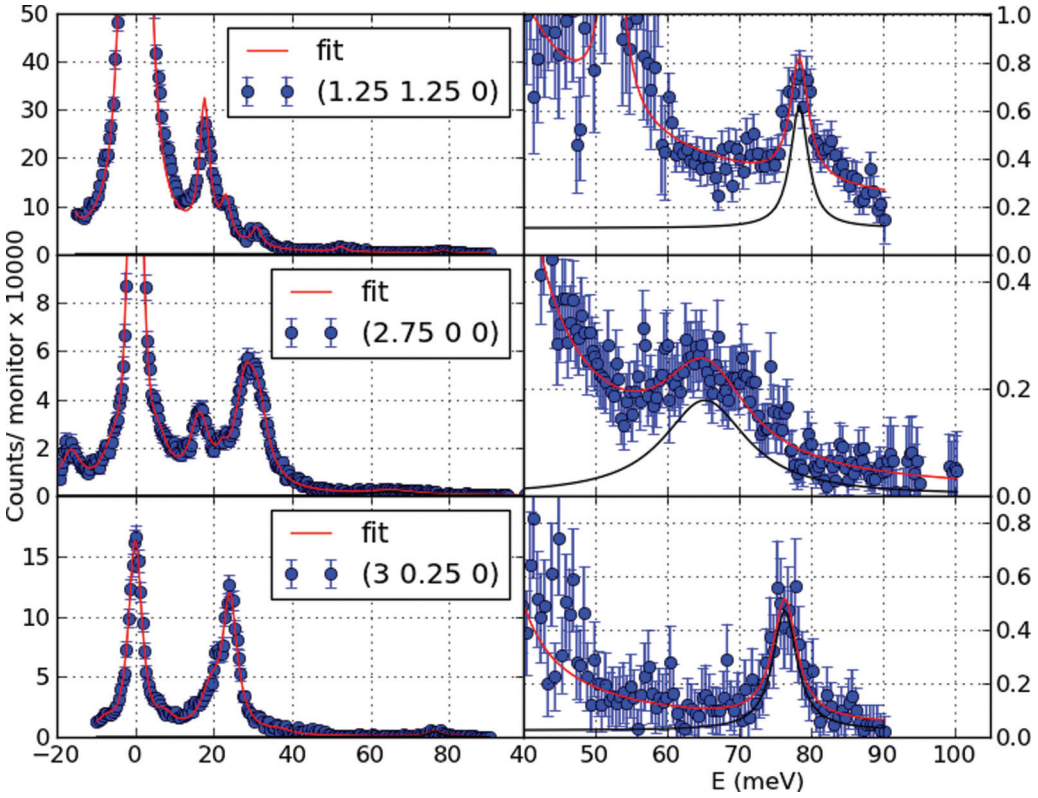

FIG. 3. (Color online) Plot[31] of the measured IXS intensities as a function of energy on $Ca_{2-x}CuO_2Cl_2$ for the propagation vector corresponding to the middle of the Brillouin zone along three different symmetry *in-plane* lines. Left column shows the overall data, while the right column shows the respective zoom at the high energy of the Cu-O bond stretching mode. (Top) Longitudinal at (0.25 0.25 0), with Σ_1 symmetry. (Middle) Longitudinal at (0.25 0 0), with Δ_1 symmetry. (Bottom) Transverse at (0 0.25 0), with Δ_3 symmetry. Red lines are fit to the data described in the text. The contribution from the Cu-O bond stretching mode is singled out as a black line.

oxygen buckling modes. The third, undoped, sample showed a mosaic too large for doing any phonon measurement. Phonons were measured from (1,1,0) to (2.2, 2.2, 0) along (1,1,0) and from (2,0,0) to (3,0,0) along (1,0,0) in longitudinal geometry, and from (3,0,0) up to (3, 0.5, 0) in transverse one.

The main monochromator was set to the Si (9 9 9) Bragg reflection, with a wavelength of 0.6968 Å (17794 eV) and an energy resolution $\Delta E = 3.0 \pm 0.2$ meV (see Ref. 26–28 for details). The back-scattered beam is focused by a platinum-coated toroidal mirror, which provided a focal spot at the sample position of 0.270 (horizontal) and 0.080 (vertical) mm^2 FWHM at the sample position. The IXS spectrometer[29] was used with a setup allowing simultaneous measurements from 5 analyzers. Analyzer slits were open to (60 × 60) mm, thus integrating over a solid angle of 0.6°, amounting to a Q resolution of ± 0.416 nm^{-1} corresponding to approximately 0.06 of the Brillouin zone along (1,0,0).

Figure 3 shows representative IXS spectra for three different directions, longitudinal along (q q 0), with Σ_1 character, longitudinal along the (q 0 0) direction, with Δ_1 character, and transverse along the equivalent (0 q 0) direction, with Δ_3 character, for the same value $q = 0.25$. Continuous lines are a model, consisting of a Lorentzian function, convoluted with the instrumental function. The model is chosen to fit the data using a χ^2 minimization procedure.[30]

In $Ca_{2-x}CuO_2Cl_2$, the contrast between the elastic line and the low-energy mode on one side and high-energy mode on the other, is not as strong as in other cuprates. The ratio is determined by the ions number of electrons, as the IXS scattering yield is proportional to Z^2 and the photoelectron absorption to Z^4, so that the high-Z elements dominate in a system with different atomic species, while the high-energy modes come almost exclusively from light element vibrations.[32,33] In other cuprate systems, measuring the high-energy mode dispersion is therefore possible only at few (∼10) degrees Kelvin, where the Bose factor is strongly reduced for modes below 25 meV, compared to the intensity at room temperature.[34] The measurements presented here are, in turn, all taken at room temperature, so that the contrast in the intensities between high and low energy is largely due to the Bose contributions, still allowing the measurements of all high-energy phonon modes.

C. Calculations

The phonon dispersion is simulated using the lattice dynamical calculation package OPENPHONON,[35] based on a shell model, further adapted for compilation with PYTHON 2.7.[36] In order to be consistent with previous studies on the phonon dispersion in cuprates by INS[14,23] and IXS,[13,37,38] we used a common potential model for cuprates, where the interatomic potentials have been derived from a comparison of the INS results for different HTcS compounds by Chaplot *et al.*.[39] In this model, a screening of the Coulomb potential is added in

TABLE I. Ion parameters of the lattice dynamical shell model described in the text.

k	$Z(k)$	$Y(k)$	$K(k)$ (nm^{-1})
O	−1.56	−3.0	1800
Cl	−0.92	−1.0	1800
Cu	1.64	3.0	2000
Ca	1.66	3.0	700

order to simulate the effect of the free carriers introduced by doping. In the same way as described by Chaplot (see Ref. 39) for metallic $La_{2-x}Sr_xCuO_4$ and $YBa_2Cu_3O_7$, we replaced the long-range Coulomb potential $V_c(q)$ by $V_c(q)/\epsilon(q)$, and for the dielectric function, we took the semiclassical Thomas-Fermi limit of $\epsilon(q) = 1 + \kappa_s^2/q^2$, where κ_s^2 indicates the screening vector. In our calculation, we estimate a screening wave number $\kappa_s = \frac{4}{a} \sim 0.4$ Å^{-1}, where a is the lattice parameter, which corresponds to a doping of about 10% according to Ref. 39. For ions and bonds not included in the previous model, we used the parameters used by Mittal *et al.*[40] for Cl and by Chaplot[41] for Ca as a starting point of our refinement. We used the experimental lattice parameters as reported in Ref. 19. The solution is stable with the set of atomic potentials found without adding any additional force constant to equilibrate the fictitious forces originating from anharmonic contributions when using real structural parameters in a quasiharmonic approximation. A summary of the ion and bond parameters are given in Tables I and II respectively. In Fig. 4, we show the main atomic displacement pattern as calculated by our model at the zone center Γ for the *in-plane* modes we have measured.

Note that, from now on, we will use the character of the mode along a particular dispersion line as a label for the line itself [e.g., Δ_1 for the line (q 0 0) in longitudinal geometry], and the zone center character as a label for the whole mode dispersion [e.g., Eu(1) along Δ_1 for the Cu-O bond stretching mode along the line (q 0 0) in longitudinal geometry].

III. RESULTS

IXS spectra show overall well defined phonon modes, in general with resolution-limited energy width, with the notable exception of the Cu-O bond stretching mode [Eu(1)] along Δ_1. They therefore present no difficulty for the fit procedure, in order to determine the phonon frequencies, width, and intensities.

The parameters obtained from the fitting of these and several other spectra are plotted in Fig. 5, for the frequency

TABLE II. Bond parameters of the lattice dynamical shell model described in the text.

k-k'	$A_{kk'}$ (eV)	$R_{kk'}$ (Å)	$C_{kk'}$ (eV Å^6)
Cu-O	4000	0.228	
Cu-Cl	4000	0.29	
O-O	2000	0.284	100
Ca-O	1600	0.304	
Cl-Cl	2000	0.34	
Ca-Cl	1600	0.33	

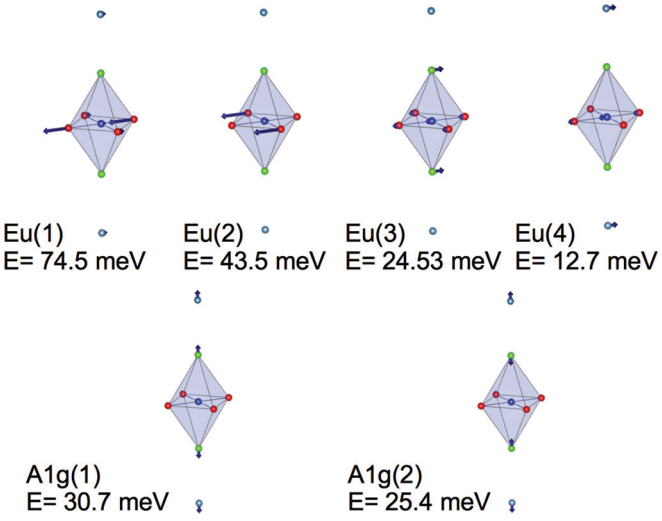

FIG. 4. (Color online) Drawing[21] of the atomic displacements of the *in-plane* modes that we have measured at the zone center Γ, as calculated by our lattice dynamical model described in the text. For each mode, we give its character, and the calculated frequency at Γ. We highlight the octahedron formed by the anions, with the two apical chlorines and the four square coordinated oxygens, around the copper, in order to single out the differences and similarities with analogue displacements in hole-doped cuprates with T structure as, e.g., shown in Ref. 24. The calcium cations lies outside the octahedron, on the vertical of the apical chlorine one.

mode dispersions, and Fig. 6, for the mode intensities. In Fig. 5, the experimental frequencies obtained by IXS are compared with the calculated dispersions. We also include experimental zone center modes estimated frequencies, obtained by infrared absorption on heavily underdoped $Ca_{2-x}Na_xCuO_2Cl_2$ ($x = 0$, 0.3) in Ref. 42. In Fig. 6, the IXS intensities are compared with the dynamical structure factor calculated using the eigenvector simulated in our model. Overall, we observe a good agreement between the measured frequencies and intensities, on one side, and the calculated ones on the other side. This with the notable exception of (1) the highest-energy optic mode, the Cu-O bond stretching, with Δ_1 symmetry, (2) a spurious intensity at very low frequency, at about 8 meV, with flat dispersion *in-plane*, (3) the dispersion for the Eu(3) mode, the Cu-O bond-bending, along Δ_1, away from the zone center, and (4) the acoustic Σ_1 mode close to the zone boundary.

The first anomaly is well known[13,14,23,37,38] and widely debated,[5,6] while the other anomalies are rather new. We discuss the details of our observation and possible interpretations in the following section. In Tables I and II, we give the ionic and bond parameters used for the model shown in Figs. 5 and 6.

Overall, the agreement between the calculated and measured dispersion is comparable to the one found using similar atomistic models[23,39] or even more advanced *ab initio* approaches.[5,14] Moreover, we find a satisfying agreement between the calculated intensities, with the experimental ones on the IXS peak with closer frequencies of the calculated dispersion. This not only supports the assignment we suggest for the phonon branches we have measured but it is also a proof of the quality of the model, as finding correct eigenvectors is a more delicate task than finding frequencies.

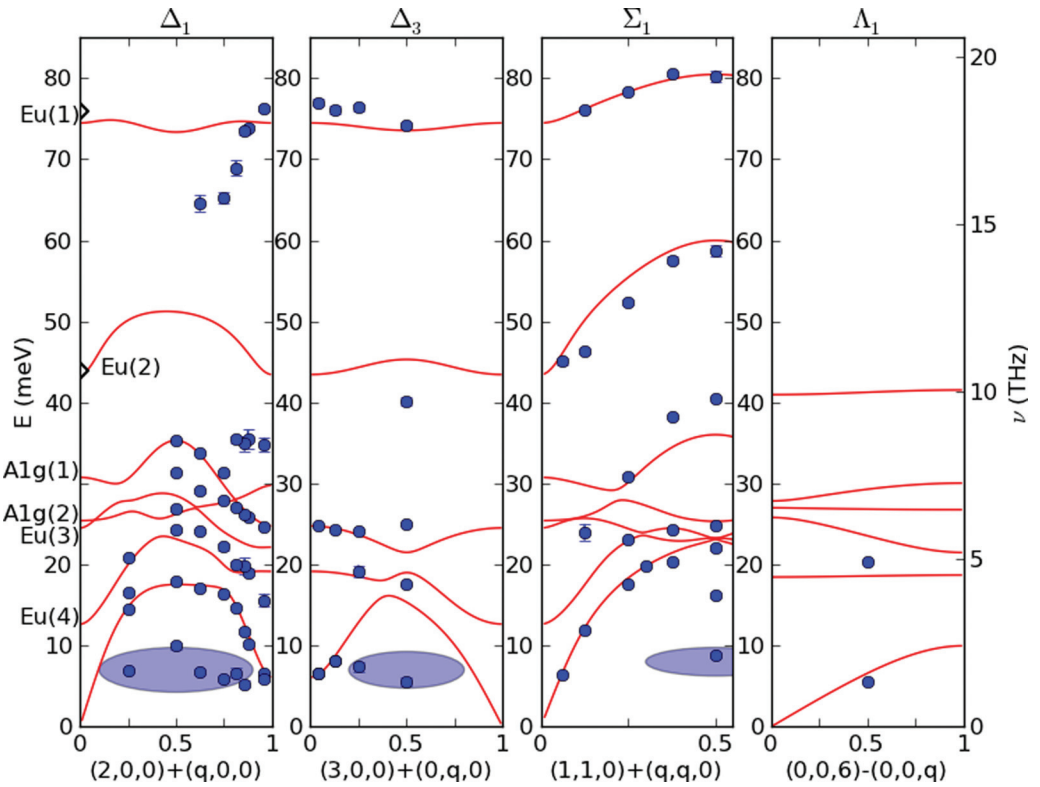

FIG. 5. (Color online) Chart[31] of the $Ca_{2-x}CuO_2Cl_2$ phonon dispersion (blue circles) measured by IXS and calculated frequencies using the shell model of lattice dynamics described in the text (red line). We also indicate, on the left panel, the frequencies at the zone center Γ, extrapolated from their positions in the infrared spectra reported in Ref. 42 (empty triangle-right).

IV. DISCUSSION

The lattice dynamical shell model has been refined only with a limited tuning of the ionic and bond parameters concerning the chlorine and calcium ions, otherwise imposing the parameters from Ref. 39, confirming that the common potential model is appropriate for the cuprates. We would like to discuss now in more details our present understanding of the discrepancies between the data and the calculations.

a. Dispersionless intensity at about 8 meV. We observe a low-energy flat mode (point 2 above) *in-plane*, mainly along the Δ_1 and Δ_3 directions. Along the Σ_1 direction, the fitting of the central line is improved if we add some intensity in the same frequency region, but it is not well resolved, with perhaps the exception of the zone boundary. The difference is possibly due to the larger intensity of the elastic line in the geometry corresponding to Σ_1 scattering, which is accidental, and therefore, we can not consider this anomalous excitation anisotropic from our data. In the Δ_1 and Δ_3 directions, it appears as a rather shallow intensity between the elastic line and the acoustic mode but with an intensity well above the background. For a few scans only, it appears with a well defined maximum. The origin of this mode is not understood at the moment but it is also observed in a closely related system for which we are presently running experimental investigations[43] in order to test different hypotheses of the nature of this additional mode, including defect vibrational states and phonon modes activated by symmetry breaking. We note also that several works using Raman scattering and infrared absorption in underdoped $La_{2-x}Sr_xCuO_{4+\delta}$[44–48] found intensity at a similar energy in an underdoped sample, which is attributed to modes related to the stripe charge modulations.

b. Acoustic Σ_1 mode close to the zone boundary. The anomaly on the Σ_1 acoustic mode close to the zone boundary concerns only one point, while the rest of the dispersion fits quite well with our simulations, both for the frequencies and the intensities. It would be nevertheless interesting to further study this mode, by complementary *ab initio* calculations, to verify our findings, as well as with more detailed measurements close to the zone boundary.

c. Cu-O bond bending mode. The calculated frequency of the Cu-O bond bending mode at the zone center Γ is very close to the experimental IR position for the corresponding Eu(2) mode, but our calculation shows an upward dispersion, which does not seem to be confirmed by our data along Δ_3. Indeed, the experimental intensity along Δ_3 between 30 and 40 meV seems to lie at a lower energy with respect to the calculated one. However, the Cu-O bond bending mode has a relatively low yield, along both Δ_1 and Δ_3, comparable to the bond-stretching one, while being at a lower energy. They are therefore measured on top of the tails of the much stronger modes at lower energy, as described above, a fact that complicates their detection. A further investigation of this dispersion along Δ_1 and Δ_3 would be possible only at low temperature, as discussed above. Note that, on the contrary, for the corresponding Eu(2) mode along Σ_1, the mode is

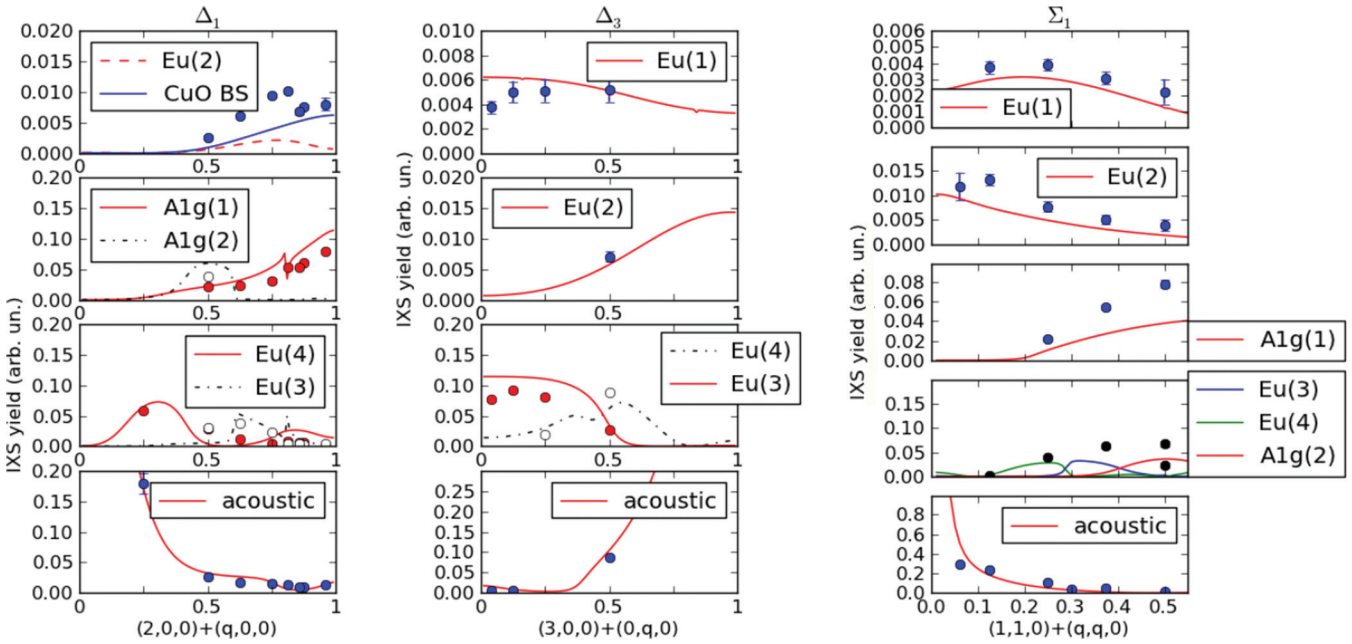

FIG. 6. (Color online) Calculated (lines) and experimental (symbols) inelastic scattering intensities for phonon modes in $Ca_{2-x}CuO_2Cl_2$ CuO, with character Δ_1 (left), Δ_3 (center), and Σ_1 (right).[31] The intensity units are arbitrary for calculations. The experimentally reported areas of peak units are in $I/I_0\times$ meV and are multiplied by a common factor for all modes for a given line in the Brillouin zone. Mode assignment is based on the closest experimental frequency to a given calculated mode. The only exception is the acoustic and(or) Eu(4) mode at $q = (3,0.5,0)$, for which both assignments are proposed (and match) the calculated one. Labels correspond to the modes character at the zone center as explained in the text.

reasonably well resolved and matches very well both the calculated frequency dispersion and the intensity.

d. Cu-O bond stretching mode. Concerning the Cu-O bond stretching along the bond direction, (q 0 0), we calculate a symmetrical dispersion in the extended zone, similarly to other cuprate with T structure. Frequencies at both zone center $q = 0$ and extended zone boundary $q = 2\frac{\pi}{a}$ are the same and do not change with doping in the systems where doping dependence is known (see, for example, Refs. 14 and 49). For such a branch, the mode has a vanishing small dynamical structure factor, so we can not compare directly the dispersion close to the zone center and $q = 2\frac{\pi}{a}$. On the other hand, IR data show a well defined phonon mode at the zone center but only in the insulating phases. We remark that the IR data assigned to the EU(1) mode on heavily underdoped samples correspond very well to the frequency we found at the zone boundary for both Δ_1 and Δ_3 Cu-O bond stretching modes. This suggests that the physics for this mode is very similar to the one of $La_{2-x}Sr_xCuO_{4+\delta}$,[14,49] despite the present lack of dispersion data in the undoped parent compound, and of mode frequencies an the zone center Γ in the doped one.

In Fig. 7, top panels, we show the details of the Cu-O bond stretching for the direction with Δ_1 (half-breathing) and Σ_1 (full-breathing) character and compare to our lattice dynamics simulations, with different screening wave number κ_s. In the same figure, bottom panel, we can follow the corresponding broadening of the mode, which starts at a value of less than 1 meV, once the instrumental resolution is subtracted, to end up at more than 12 meV. Note that the softening and simultaneous broadening is observed only for the mode with character Δ_1 propagating along (q00) (Fig. 7, left, top, and bottom). The same mode propagating along the diagonal (Σ_1, Fig. 7, left) is dispersing upward, with a line shape that is resolution limited, as in other cuprates.[14]

STM experiments in oxychlorides[20] report a modulation of the Fourier transform of the differential conductance map $g(\mathbf{r},E)$ at wave vectors of (nq, 0 0) with n integer and $q \sim 0.25$, i.e., for modulations with a periodicity corresponding to $4a$. This is reminiscent of what happens in cuprates[14,15] and other perovskite-like ternary transition metal oxides,[50] with the difference that in oxychlorides, there is no observation of static diffraction by charge density modulation. We can then confirm that the observation of STM has a dynamical precursor at room temperature, similar to the stripes in other cuprates. Note that the pattern observed by STM was first labeled as "checkerboard",[20] although this was not confirmed by further studies[51] that maintained, however, a Cu-O-Cu bond-centered electronic pattern without long-range order but with four-lattice-constant-wide unidirectional electronic domains.[51] Indeed, for a checkerboard pattern, we should have observed the same phonon anomaly along both the Δ_1 and the Σ_1 directions, as it is the case in those transition metal oxides where such a modulation is present.[50] Here, we observe the anomaly only for the mode with Δ_1 character, which is in agreement with other cuprates showing a stripe charge modulation pattern.[14,15]

Regardless of the exact pattern of the charge modulation, we note that such anomaly can not be accounted for in simple models based on Fermi-liquid band type as the DFT ones,[15] as the charge modulations themselves can not be simulated in such theoretical framework. We remark also that the propagation vector (n0.25 0 0) of these unidirectional

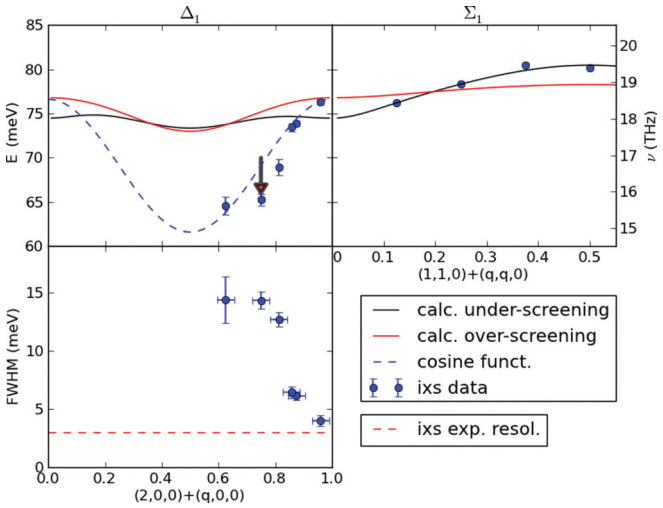

FIG. 7. (Color online) (Top) $Ca_{2-x}CuO_2Cl_2$ Cu-O bond-stretching dispersions (blue circles) measured by IXS and calculated frequencies using a shell model of lattice dynamics; (top, left) along (q 0 0) (Δ_1) and (top, right) along (q q 0) (Σ_1). Black lines corresponds to a model with lower doping and a screening wave number $\kappa_s = \frac{\pi}{2a}$, while red lines corresponds to a model with higher doping, and a screening wave number $\kappa_s = \frac{\pi}{a}$. The blue dashed line is a cosine function compared to the data of Δ_1 symmetry in order to show the marked anomaly at $q \sim 0.75$. Bottom panel: Blue full circles are the FWHM of the IXS data corresponding to the Cu-O bond-stretching mode along (q 0 0), showing a maximum around $q \sim 0.75$.[31]

electronic domains, where we observe the "sharp dip" anomaly (see Fig. 7), would correspond to a nesting vector of the Fermi surface, as reported for Na-doped $Ca_2CuO_2Cl_2$,[52] although the region of the Fermi surface connected by this vector does not show well defined *quasiparticles*.

Apart from this peculiar anomaly close to the charge-modulation wave vector ($\pi/2a$ 0 0), it has been claimed that the overall bending down of the mode with Δ_1 character is well reproduced by DFT calculations,[4,5,7] which reproduce a smooth cosine function shape. These calculations found that such mode has one of the highest couplings with charge carriers. Nevertheless, the calculated electron-phonon coupling was still too low to account for the strong kink in ARPES dispersion,[5] and the very high T_c of cuprates.[4] Moreover, similar calculations showed a concurrent strong downward bending of the Σ_1 mode, which can lead to discrepancies at the zone boundary X (π/a π/a 0) between calculated and experimental frequencies in optimal or slightly underdoped compounds up to 10 meV.[4,7] It was suggested that such a difference originates from unrelated effects over the two directions (q 0 0) and (q q 0).[4] Note that Giustino and co-workers in Ref. 5 use the label *half-breathing* and *full-breathing* to distinguish Cu-O bond-stretching modes with different character, as in other works,[49] but the *full-breathing* label is not consistent throughout the literature, as it indicates modes with Σ_1 character in Ref. 49, while misleadingly labels a dispersion along (q 0 0) with Δ_3 character in Ref. 5. It is worthwhile to notice that the later dispersion has been found to be flat for all dopings, either experimentally or theoretically. At the same time, the authors of Ref. 5 do not show their results along Σ_1, where a very bad agreement is found in other DFT calculations[4,7] and experimental data. We therefore avoid the "breathing" notation.

Contrary to DFT simulations, our simple lattice dynamical calculation, based on a shell model, reproduces well the dispersion of the mode with Σ_1 character, while it is missing the softening of the one with Δ_1 character when using a screening wave number of $\kappa_s = \frac{\pi}{2a}$ (see Fig. 7). When we increase the doping, and consequently the screening wave number, we observe a modest softening for both bands. The effect is relatively weak in our calculations, as we have kept all other parameters fixed, in order to allow a direct comparison between the two cases. The important point here is that the softening affects exclusively the modes with Δ_1 and Σ_1 character, with a trend that reproduces the experimental one with increasing doping. This suggests that overestimated screening effects can lead to simulations that reproduce the dispersion at much higher doping. If compared to optimal or slightly underdoped compounds, this gives a dispersion that is accidentally similar to the one for the mode with Δ_1 character while giving a large difference between calculation and experimental dispersion for the mode with Σ_1 character, and accordingly underestimates the electron-phonon coupling. Indeed, the dispersion found in Refs. 4 and 5 for the Cu-O bond-stretching modes with Δ_1 and Σ_1 character is strikingly similar to the experimental dispersion found only in the highly overdoped cuprates $La_{2-x}M_xCuO_4$ (M = Sr,Ba).[13,49] Therefore a possible unique origin for the softening of modes with both Δ_1 and Σ_1 character in DFT calculations can not be ruled out. This would imply that the phonon simulations by DFT correspond to a much higher doping, which, because of the larger screening, have a lower electron-phonon coupling. To confirm such conclusion also in oxychlorides, it would be important to compare with DFT calculations and to have data on the undoped parent compound.

V. CONCLUSIONS

We presented an extended study of the phonon dispersion in superconducting $Ca_{2-x}CuO_2Cl_2$, doped with Ca vacancies, close to optimal doping. We interpret the results using lattice dynamical calculations based on a shell model, and we compare them to what was obtained for other hole-doped cuprates, in particular, with the T structure. We found an overall agreement between our model and the data, confirming the good choice of parameters of the common interatomic potential for the lattice dynamics of cuprates proposed in Ref. 39. An anomalous dip in the Cu-O bond stretching dispersion develops also in oxychlorides with a simultaneous marked broadening of the mode. The broadening maximum appears at $\approx[\pi/(2a)$ 0 0], which corresponds to the charge-modulation propagation vector, observed by means of STM experiments.[20] Our data thus unveil a dynamic precursor state of the above modulations. By comparing our measurements on the longitudinal Cu-O bond-stretching mode in superconducting $Ca_{2-x}CuO_2Cl_2$ with our model, we found that the screening effect may bend downwards simultaneously the dispersions along the (q 0 0) and (q q 0) directions, a result that can help explain the discrepancies between phonon dispersions based on DFT calculations[4,7] and the experimental data in cuprates.

ACKNOWLEDGMENTS

We are very grateful to M. Calandra and F. Mauri for useful discussion. We also thank S. Chaplot and M. Rao for encouraging exchanges and suggestions and R. Heid and T. Hanaguri for enlightening discussions and critical reading of the manuscript. We acknowledge D. Gambetti and B. Baptiste for technical help during measurements and A. Shukla for redaction suggestions. This work was supported by ESRF through Experiment No. HS-3461. I.Y. gratefully acknowledges the European Commission for financial support under Contract MIIF-CT-2006-0374.

*matteo.dastuto@impmc.upmc.fr

†Present address: Nanoscience and Nanotechnology Research Center (N2RC), Research Institutes for the Twenty-First Century - Osaka Prefecture University 1-2 Gakuen-cho, Naka-ku, Sakai, Osaka 599-8570, Japan.

‡Present address: Diamond Light Source, Didcot OX11 0DE, United Kingdom.

[1] J. G. Bednorz and K. A. Müller, Z. Phys. B **64**, 189 (1986).

[2] M. K. Crawford, W. E. Farneth, E. M. McCarronn, R. L. Harlow, and A. H. Moudden, Science **250**, 1390 (1990).

[3] D. A. Bonn, Nat. Phys. **2**, 158 (2006).

[4] K.-P. Bohnen, R. Heid, and M. Krauss, Europhys. Lett. **64**, 104 (2003).

[5] F. Giustino, M. L. Cohen, and S. G. Louie, Nature (London) **452**, 975 (2008).

[6] O. Rösch and O. Gunnarsson, Phys. Rev. Lett. **93**, 237001 (2004).

[7] C. Falter, T. Bauer, and F. Schnetgöke, Phys. Rev. B **73**, 224502 (2006).

[8] J. M. Tranquada, B. J. Sternlieb, J. D. Axe, Y. Nakamura, and S. Uchida, Nature (London) **375**, 561 (1995).

[9] P. Abbamonte, A. Rusydi, S. Smadici, G. Gu, G. Sawatzky, and D. Feng, Nat. Phys. **1**, 155 (2005).

[10] R. J. McQueeney, Y. Petrov, T. Egami, M. Yethiraj, G. Shirane, and Y. Endoh, Phys. Rev. Lett. **82**, 628 (1999).

[11] L. Pintschovius and M. Braden, Phys. Rev. B **60**, R15039 (1999).

[12] D. Reznik, L. Pitschovius, M. Ito, S. Iikubo, M. Sato, H. Goka, M. Fujita, K. Yamada, G. Gu, and J. Tranquada, Nature (London) **440**, 1170 (2006).

[13] M. d'Astuto, G. Dhalenne, J. Graf, M. Hoesch, P. Giura, M. Krisch, P. Berthet, A. Lanzara, and A. Shukla, Phys. Rev. B **78**, 140511(R) (2008).

[14] D. Reznik, Adv. Condens. Matter. Phys. **2010**, 523549 (2010).

[15] D. Reznik, G. Sangiovanni, O. Gunnarsson, and T. P. Devereaux, Nature (London) **455**, E6 (2008).

[16] W. H. Butler, H. G. Smith, and N. Wakabayashi, Phys. Rev. Lett. **39**, 1004 (1977).

[17] F. Weber, S. Rosenkranz, L. Pintschovius, J.-P. Castellan, R. Osborn, W. Reichardt, R. Heid, K.-P. Bohnen, E. A. Goremychkin, A. Kreyssig, K. Hradil, and D. L. Abernathy, Phys. Rev. Lett. **109**, 057001 (2012).

[18] Z. Hiroi, N. Kobayashi, and M. Takano, Nature (London) **371**, 139 (2002).

[19] I. Yamada, A. A. Belik, M. Azuma, S. Harjo, T. Kamiyama, Y. Shimakawa, and M. Takano, Phys. Rev. B **72**, 224503 (2005).

[20] T. Hanaguri, C. Lupien, Y. Kohsaka, D.-H. Lee, M. Azuma, M. Takano, H. Takagi, and J. C. Davis, Nature (London) **430**, 1001 (2004).

[21] K. Momma and F. Izumi, J. Appl. Crystallogr. **41**, 653 (2008).

[22] I. Yamada, M. Azuma, Y. Shimakawa, and M. Takano, Physica C **460-462**, 420 (2007).

[23] L. Pintschovius and W. Reichardt, in *Physics and Chemistry of Materials with Low-Dimensional Structures*, edited by A. Furrer (Kluwer Academic Publishers, Dordrecht, 1998), Vol. 20, p. 165.

[24] S. Tajima, T. Ido, S. Ishibashi, T. Itoh, H. Eisaki, Y. Mizuo, T. Arima, H. Takagi, and S. Uchida, Phys. Rev. B **43**, 10496 (1991).

[25] Data plot and fit obtained using IGOR PRO (Wavemetrics, Lake Oswego, OR, USA).

[26] M. Krisch and F. Sette, in *Light Scattering in Solid IX*, Topics in Applied Physics, Vol. 108, edited by M. Cardona and R. Merlin (Springer, Berlin, Heidelberg, 2007), pp. 317–370.

[27] R. Verbeni, F. Sette, M. Krisch, U. Bergmann, B. Gorges, C. Halcoussis, K. Martel, C. Masciovecchio, J. Ribois, G. Ruocco, and H. Sinn, J. Synchrotron Radiat. **3**, 62 (1996).

[28] R. Verbeni, M. d'Astuto, M. Krisch, M. Lorenzen, A. Mermet, G. Monaco, H. Requardt, and F. Sette, Rev. Sci. Instrum. **79**, 083902 (2008).

[29] C. Masciovecchio, U. Bergmann, M. Krisch, G. Ruocco, F. Sette, and R. Verbeni, Nucl. Instrum. Meth. B **111**, 181 (1996).

[30] F. James, *MINUIT Function Minimization and Error Analysis*, Computing and Networks Division, CERN, Geneva, 1998 (CERN D506 Long Writeup).

[31] Graphics obtained using MATPLOTLIB (Ref. 33), freely available on http://matplotlib.org/.

[32] M. d'Astuto and M. Krisch, JDN **10**, 487 (2010).

[33] J. D. Hunter, Comput. Sci. Eng. **9**, 90 (2007).

[34] M. d'Astuto, P. K. Mang, P. Giura, A. Shukla, A. Mirone, M. Krisch, F. Sette, P. Ghigna, M. Braden, and M. Greven, Int. J. Mod. Phys. B **17**, 484 (2003).

[35] A. Mirone, OPENPHONON code source (2001), http://sourceforge.net/projects/openphonon/.

[36] L. Paulatto, A. Mirone, and M. d'Astuto (private communication).

[37] M. d'Astuto, P. K. Mang, P. Giura, A. Shukla, P. Ghigna, A. Mirone, M. Braden, M. Greven, M. Krisch, and F. Sette, Phys. Rev. Lett. **88**, 167002 (2002).

[38] M. d'Astuto, A. Mirone, P. Giura, D. Colson, A. Forget, and M. Krisch, J. Phys.: Condens. Matter **15**, 8827 (2003).

[39] S. L. Chaplot, W. Reichardt, L. Pintschovius, and N. Pyka, Phys. Rev. B **52**, 7230 (1995).

[40] R. Mittal, S. L. Chaplot, A. Sen, S. N. Achary, and A. K. Tyagi, Phys. Rev. B **67**, 134303 (2003).

[41] S. L. Chaplot, Phys. Rev. B **37**, 7435 (1988).

[42] Y. Zenitani, H. Kawashima, T. Suzuki, J. Akimitsu, N. Ogita, T. Kondo, and M. Udagawa, J. Phys. Soc. Jpn. **74**, 1877 (2005).

[43] M. d'Astuto and D. Lamago (private communication).

[44] L. Tassini, F. Venturini, Q.-M. Zhang, R. Hackl, N. Kikugawa, and T. Fujita, Phys. Rev. Lett. **95**, 117002 (2005).

[45]S. Sugai, Y. Takayanagi, and N. Hayamizu, Phys. Rev. Lett. **96**, 137003 (2006).
[46]S. Caprara, C. Di Castro, M. Grilli, and D. Suppa, Phys. Rev. Lett. **95**, 117004 (2005).
[47]A. Lucarelli, S. Lupi, M. Ortolani, P. Calvani, P. Maselli, M. Capizzi, P. Giura, H. Eisaki, N. Kikugawa, T. Fujita, M. Fujita, and K. Yamada, Phys. Rev. Lett. **90**, 037002 (2003).
[48]F. Venturini, Q.-M. Zhang, R. Hackl, A. Lucarelli, S. Lupi, M. Ortolani, P. Calvani, N. Kikugawa, and T. Fujita, Phys. Rev. B **66**, 060502 (2002).
[49]L. Pintschovius, D. Reznik, and K. Yamada, Phys. Rev. B **74**, 174514 (2006).
[50]F. Weber, N. Aliouane, H. Zheng, J. F. Mitchell, D. N. Argyriou, and D. Reznik, Nat. Mater. **8**, 798 (2009).
[51]Y. Kohsaka, C. Taylor, K. Fujita, A. Schmidt, C. Lupien, T. Hanaguri, M. Azuma, M. Takano, H. Eisaki, H. Takagi, S. Uchida, and J. C. Davis, Science **315**, 1380 (2007).
[52]K. M. Shen, F. Ronning, D. H. Lu, F. Baumberger, N. J. C. Ingle, W. S. Lee, W. Meevasana, Y. Kohsaka, M. Azuma, M. Takano, H. Takagi, and Z.-X. Shen, Science **307**, 901 (2005).